Mercadelli, E.; Gondolini, A.; Montaleone, D.; Pinasco, P.; Escolástico Rozalén, S.; Serra Alfaro, JM.; Sanson, A. (2020). Production strategies of asymmetric BaCe0.65Zr0.20Y0.15O3-delta - Ce(0.8)Gd(0.2)O(2-delta) membrane for hydrogen separation. International Journal of Hydrogen Energy. 45(12):7468-7478. https://doi.org/10.1016/j.ijhydene.2019.03.148

Production strategies of asymmetric $BaCe_{0.65}Zr_{0.20}Y_{0.15}O_{3-\delta}$ - $Ce_{0.8}Gd_{0.2}O_{2-\delta}$ membrane for hydrogen separation

Elisa Mercadelli[a*], Angela Gondolini[a], Daniel Montaleone[a], Paola Pinasco[a], Sonia Escolástico[b], José M. Serra[b], Alessandra Sanson[a]

[a] Institute of Science and Technology for Ceramics, National Council of Research (ISTEC-CNR), Via Granarolo 64, 48018, Faenza, Italy

[b] Instituto de Tecnología Química (Universitat Politècnica de València-Consejo Superior de Investigaciones Cientificas), Av. Los Naranjos s/n, E-46022 Valencia, Spain

* Corresponding author: elisa.mercadelli@istec.cnr.it, Tel.: +39 0546699743, fax: +390546 46381

Abstract

Mixed proton and electron conductor ceramic composites are among the most promising materials for hydrogen separation membrane technology especially if designed in an asymmetrical configuration (thin membrane supported onto a thicker porous substrate). However a precise processing optimization is needed in order to effectively obtain planar and crack free asymmetrical membranes with suitable microstructure and composition without affecting their hydrogen separation efficiency. This work highlights for the first time the most critical issues linked to the tape casting process used to obtain $BaCe_{0.65}Zr_{0.20}Y_{0.15}O_{3-\delta}$ - $Ce_{0.8}Gd_{0.2}O_{2-\delta}$ (BCZY-GDC) asymmetrical membranes for H_2 separation. The critical role of the co-firing process, sintering aid and atmosphere was critically investigated. The optimization of the production strategy allowed to obtain asymmetric membranes constituted by a dense 20 μm-thick ceramic-ceramic composite layer supported by a porous (36 %) 750 μm-thick BCZY-GDC substrate. The asymmetric membranes here reported showed H_2 fluxes (0.47 mL min^{-1} cm^{-2} at 750°C) among the highest obtained for an all-ceramic membrane.

Keywords

Tape casting; BCZY-GDC; ceramic membranes; microstructure

Introduction

Considering the limited fossil fuel reserves and the environmental concerns related to them, a transition to a sustainable and cleaner energy system is vital. In this respect hydrogen as energy vector will be a fundamental key enabling technology. On a short-term period, the intensification and optimization of hydrogen-based technologies that make use of fossil fuel as feedstock could rapidly boost this revolution [1].

However, the main product obtained by these processes is syngas, therefore to obtain pure H_2 a separation step is mandatory [2]. In this context, H_2 permeation membranes based on Mixed Proton-Electron Conductor ceramics (MPEC) [3-8], thanks to their high chemical and thermal stability, represent one of the most promising alternative to be easily integrated in pre-existent plants [9-10]. Among the MPEC ceramic membranes tested so far, dense composites of doped barium cerate or cerate-zirconate perovskites (proton conducting phase) and doped-ceria fluorite oxides (electronic conducting phase) were explored by different groups, reporting promising permeation values [11-14]. In particular, ceramic-ceramic (cer-cer) composites of $BaCe_{0.65}Zr_{0.20}Y_{0.15}O_{3-\delta}$ and $Ce_{0.8}Gd_{0.2}O_{2-\delta}$ (BCZY-GDC) have shown high robustness towards CO_2-containing atmospheres under operating conditions [15]. In addition, while Pd and Pd alloys membranes are severely deteriorated by sulfur in some cases even in the concentration range of a few ppm, it has been recently demonstrated that BCZY-GDC composite membranes show an acceptable stability under 700 ppm of H_2S, and could be therefore attractive for tailored applications such as operations related to steam reforming of methane that often contain 10–300 ppm of H_2S [16].

Nevertheless, their efficiency is still too low (H_2 flux of 0.27 mL min^{-1} cm^{-2} at 755 °C [15]) to rival Pd or ceramic-metal composites.

As postulated by the Wagner equation, the performance of the membrane in terms of hydrogen flux not only depends on the ambipolar conductivity of the material, but it is also related to the thickness of the membrane. A practical expedient to enhance the membranes performance is to reduce their thickness considering an asymmetrical architecture. When permeation across the membrane is controlled by transport through the solid phase and not by boundary layer transport or by H_2 exchange at membrane surface, the permeation rates are in fact inversely proportional to the thickness of the membrane [17]. Therefore, membranes consisting of dense films supported on porous substrates (asymmetric configuration) should lead to much higher permeation rates than the thicker structures currently used.

The production of dense-porous ceramic architectures is not however easy and required an high level of design and engineering [18-19]. This work aims to highlight and solve all the most critical issues linked to the tape casting process used to obtain asymmetrical membranes with the suitable microstructure required for H_2 separation. The critical role of co-firing process, sintering aid, and the barium-source during sintering will be exhaustively investigated and discussed. The shaping parameters will be optimized to allow the production of a planar, defect-free BCZY-GDC 20 μm-thick dense layer supported onto a 600-800 μm thick porous substrate of the same composition. Hydrogen permeability tests onto the as-prepared membranes will be finally presented.

Experimental

The steps of the process used for the membrane fabrication are schematized in Figure 1, while the detailed description of materials and procedures used for the membranes production are reported hereafter.

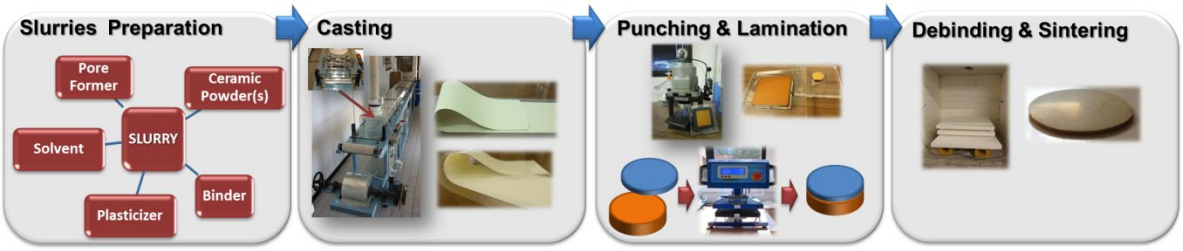

Figure 1 Schematic representation of the production process used to obtain the ceramic membranes.

For the production of the porous substrate, BCZY ($BaCe_{0.65}Zr_{0.20}Y_{0.15}O_{3-\delta}$, Specific Surface Area (SSA) = 5.8 m^2/g), supplied by Marion Technology and GDC powders ($Gd_{0.2}Ce_{0.8}O_{2-\delta}$, SSA = 6.8 m^2/g, supplied by FuelCellMaterials (USA) in a ratio equal to 50/50 vol %, were used as starting material. Rice Starch (RS, Fluka, Germany), with average particle size of 5-6 μm was used as sacrificial pore forming agent.

On the other hand, BCZY (SSA = 12.2 m^2/g, supplied by Marion Technology) and GDC powders in a ratio equal to 50/50 vol % were used for the production of the dense membrane. ZnO (Sigma Aldrich) was directly added into the tape casting suspension to promote the membrane densification. The total amount of the sintering aid was varied between 0.7 and 2 wt %.

The slurries were prepared following the standard colloidal processing technique already described elsewhere [20]. The composition of the green layer to produce the dense membrane are reported in Table 1.

Table 1 Composition of the green tape to obtain the dense layer.

	Dense membrane
Component	***(Vol %)***
Ceramic powder (BCZY+GDC)	38.3
Deflocculant	4.1
Binder	29.1
Plasticizer	28.5

On the contrary, the formulations of the porous support were optimized in terms of pore former amount, solid loading and organic content, i.e. deflocculant (glycerinetrioleate (GTO), Fluka), binder (Butvar B98, Monsanto Co., St Louis, MO, USA) and plasticizer (Santicizer 160 Monsanto Co., St Louis, MO, USA) following the logic procedure indicated in a previous work [21].

The green tapes were finally punched in discs of 24 mm in diameter. An uniaxial warm press was used to laminate the green tape layers to produce the asymmetrical BCZY-GDC bilayers. The two discs were stacked between polished parallel steel plates and heated at 55°C applying a pressure of 0.7 bar.

The bilayers were finally debinded and sintered at 1550 °C for four hours. Two different powder systems were used as sources of barium during sintering: BCZY and a 50/50 vol% mixture of BCZY-GDC following the experimental set-up already reported in a recent work [22].

Characterization

The microstructure of the sintered membranes was investigated by scanning electron microscopy (SEM-FEG, Carl Zeiss Sigma NTS GmbH, Oberkochen, Germany), embedding the cross sections under vacuum in epoxy resin and then polishing them down to 0.25 μm finish.

To check the composition of the cer-cer membrane layer, XRD analyses were performed on the dense surface at room temperature using a Bruker D8 Advance diffractometer (Bruker AXS GmbH, Karlsruhe, Germany) on a Bragg-Brentano geometry with an X-ray tube operating at 40 kV and 40 mA. Data were collected through a one-dimensional LynkEye detector based on silicon strip technology, set to discriminate Cu Kα1,2 radiation, in the 10-80° 2θ measuring range, with an equivalent counting time of 10s per 0.02° 2θ step anode X-ray.

The residual porosity of the active membrane layer was determined by image analysis of the polished cross-sections using the software ImageJ while the porosity of the porous substrate was evaluated by Hg intrusion (Pascal 140 and 240 series, Thermo Finnigan, Waltham, MA, USA).

Permeation measurements were performed on a double chamber quartz reactor following the procedure previously reported [23,24]. Argon was used on the permeate side as sweep gas (150 $mL \cdot min^{-1}$) whereas a mixture of H_2-He (100 $mL \cdot min^{-1}$) was fed to the retentate side. Measurements were performed with the membrane layer and the support on the feed and the sweep side, respectively. The dense layer of each membrane was coated by screen-printing a 20 mm thick Pt layer, while the porous support was catalytically activated by the deposition of Pt nanoparticles obtained by infiltrating a Pt precursor solution followed by a treatment at 900°C for two hours in air. Sealing was accomplished using a silver based alloy ring.

Permeation measurements were performed under both membrane sides humidified (pH_2O=0.025 atm). The H_2 content in the permeate side was analyzed using a micro-GC Varian CP-4900 equipped with Molsieve5A and PoraPlot-Q glass capillary modules. He was also continuously monitored to evaluate the leaks in the system. GC analyses were performed after 30 minutes of stabilization in the steady state and each condition was analyzed three times. H_2 fluxes ($mL \cdot min^{-1} \cdot cm^{-2}$) were calculated at standard conditions.

Results and Discussion

In order to obtain crack-free BCZY-GDC asymmetric membranes with the best compromise between the porosity of the support and the density of the membrane layer, three processing parameters were evaluated: porous support shrinkage, amount of ZnO used in the membrane layer, type of barium-source used during sintering. The influence of all these parameters on the characteristic of the final membrane is described as follows.

1. *Effect of the porous support shrinkage on the densification of the membrane layer.*

Deibert et al. [25] showed that the densification of a $La_{5.4}WO_{12-\delta}$ membrane layer is improved when it is coupled with a porous support thanks to the simultaneously shrinking of the porous layer

during sintering, known as “co-firing effect”. Similarly, Zhan et al. [26] evaluated the effect of the support composition on the shrinkage of asymmetric $SrCe_{0.95}Y_{0.05}O_{3-\delta}$ membranes. Therefore, this work aimed at correlating the composition of the supporting tape with its shrinkage during thermal treatments that affected both the final support porosity and the membrane density.

Different compositions for the BCZY-GDC supporting tapes were formulated in order to optimize the co-firing process (Table 1). The supporting BCZY tape formulation previously optimized [27,22] was used as reference for the first composition (Tape 1) only substituting half volume of BCZY with GDC, in order to obtain in the support the same mixture of the membrane (50-50 vol. %). Unfortunately, organic phase separation was clearly observed during the drying step (Figure 2a), that generated cracks and defects in the membrane body just after the organics’ burnout (Figure 2b). This effect is ascribable to an excess of the organics fraction, particularly of plasticizer which, in presence of a different inorganic matrix than BCZY, may exceed its solubility limit in the PVB polymeric network.

Modifications of the BCZY-GDC tapes formulation were therefore mandatory to obtain crack-free samples after thermal treatments. In this direction, Tape 2 was reformulated decreasing the content of both organics of Tape 1 (binder and plasticizer) by 30 vol. %, while in Tape 3 the binder and plasticizer amount was lowered by 30 vol. % and 40 vol. % respectively (Table 1).

Table 1 Volume composition of the green supporting tapes (vol. %) and properties (shrinkage, support porosity, membrane density) of the membranes sintered at 1550°C for four hours.

Tape	Powder (vol. %)	Organics (vol. %)	Pore Former (vol. %)	Shrinkage (%)	Support Porosity (%)	Membrane Density (%)
1	25.2	58.0	16.8	-	-	-
2	30.5	49.2	20.3	24.7 ± 0.1	29.4 ± 2.3	87.1 ± 0.8
3	31.9	46.8	21.3	24.6 ± 0.2	29.5 ± 2.5	87.0 ± 0.7
4	25.6	52.7	21.7	27.5 ± 0.2	25.4 ± 2.9	98.3 ± 0.6
5	25.6	47.4	27.0	26.7 ± 0.4	35.3 ± 3.8	99.0 ± 0.5
6	25.6	45.0	29.4	26.3 ± 0.2	34.9 ± 3.6	98.9 ± 0.3
7	23.8	48.9	27.3	27.1 ± 0.1	36.2 ± 3.2	99.2 ± 0.3

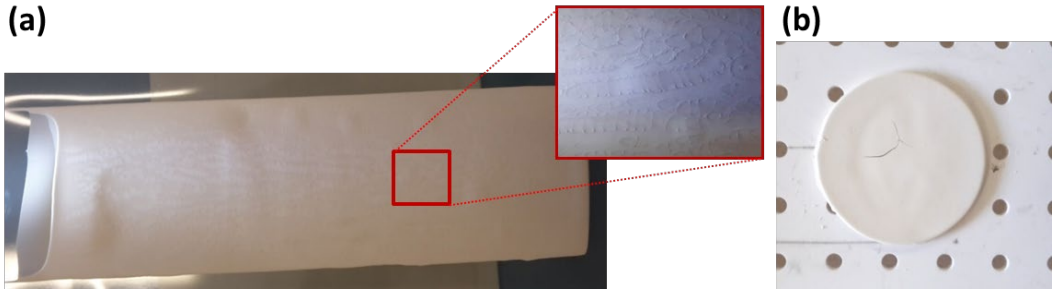

Figure 2 Picture of the green BCZY-GDC tape, formulation 1 (a) and of the corresponding as-debinded membrane (b).

Unfortunately even if planar and crack free membranes were obtained using tape 2 and tape 3, the membrane layers result not sufficiently densified as shown by SEM analyses in Figure 3 and the porosity data summarized in Table 1. It is worth noticing that the BCZY-supported samples showed a complete dense membrane layer when sintered at the same conditions [13,16]. This behaviour is ascribed to the higher shrinkage of the BCZY-supported membrane (26.3 %) in comparison to the BCZY-GDC-supported one (24.6%), thus confirming the key role of the co-firing process on the final microstructure. For this reason the green tapes formulation of the porous BCZY-GDC support was interactively modified in terms of pore former and organics amount, in order to achieve the desired microstructure (Tapes 4-7, Table 1)

As summarized in Table 1, the shrinkage of the membranes depends on the synergic effects of the three components of the slurry, i.e. solid loading, organics and pore former content, that in turn affects the resulting membrane microstructures (Figure 3).

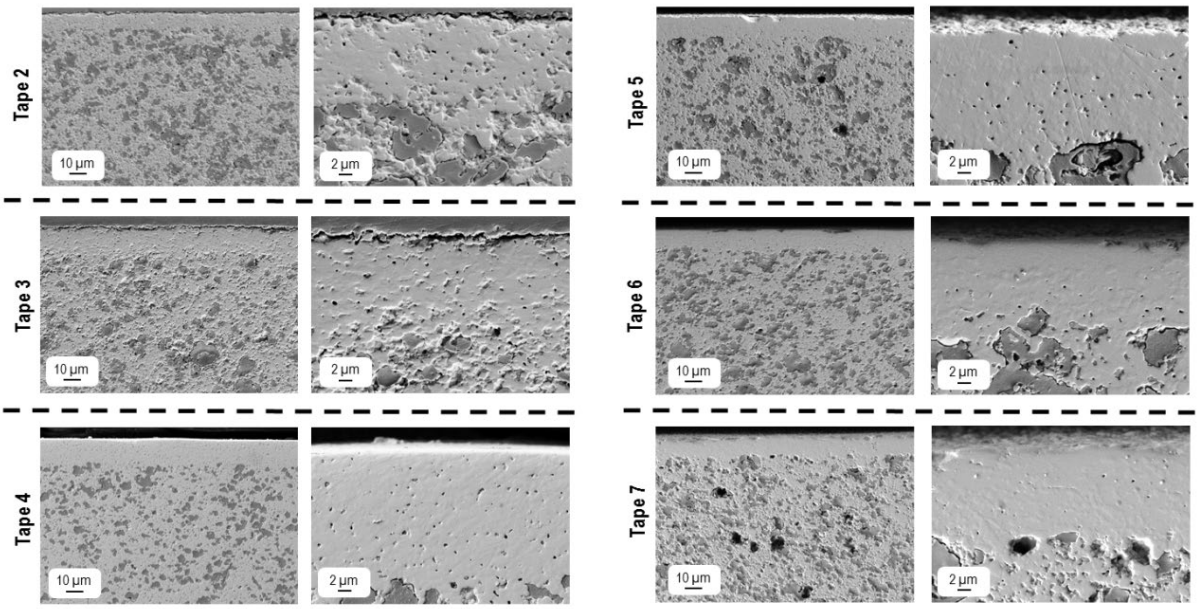

Figure 3 SEM micrographs of the polished cross-sections of the membranes sintered at 1550°C for four hours changing the formulation of the porous supports.

The data collected can be summarized by ternary diagrams (Figure 4) of the tapes formulation as a function of the shrinkage, the porosity of the substrate and the density of the membrane layer. In particular:

- Tape 2 and 3 displayed the lower shrinkage for the low organics content and high solid fraction. The lower amount of pore former hindered the porosity of the support layer, while the membrane layer had a low density value as a consequence of the low shrinkage percentage, according to the "co-firing effect" previously mentioned.
- The high organics content of the Tape 4 promoted the shrinkage, and consequently the densification of the membrane layer. On the other hand, the low fraction of pore former limited the support porosity.
- Tape 5 and 6 showed a good shrinkage percentage which led to a good densified membrane layer. Comparing the two formulations, the higher the organics content, the higher the shrinkage; while the higher the pore former fraction, the higher the support porosity. This means that the small

porosity led by the binder and plasticizer burn-out after the debinding is removed during sintering increasing the shrinkage of the membrane.

- Tape 7 displayed the highest support porosity and the highest densification of the membrane layer thanks to its optimized formulation and balance between organics/pore former contents.

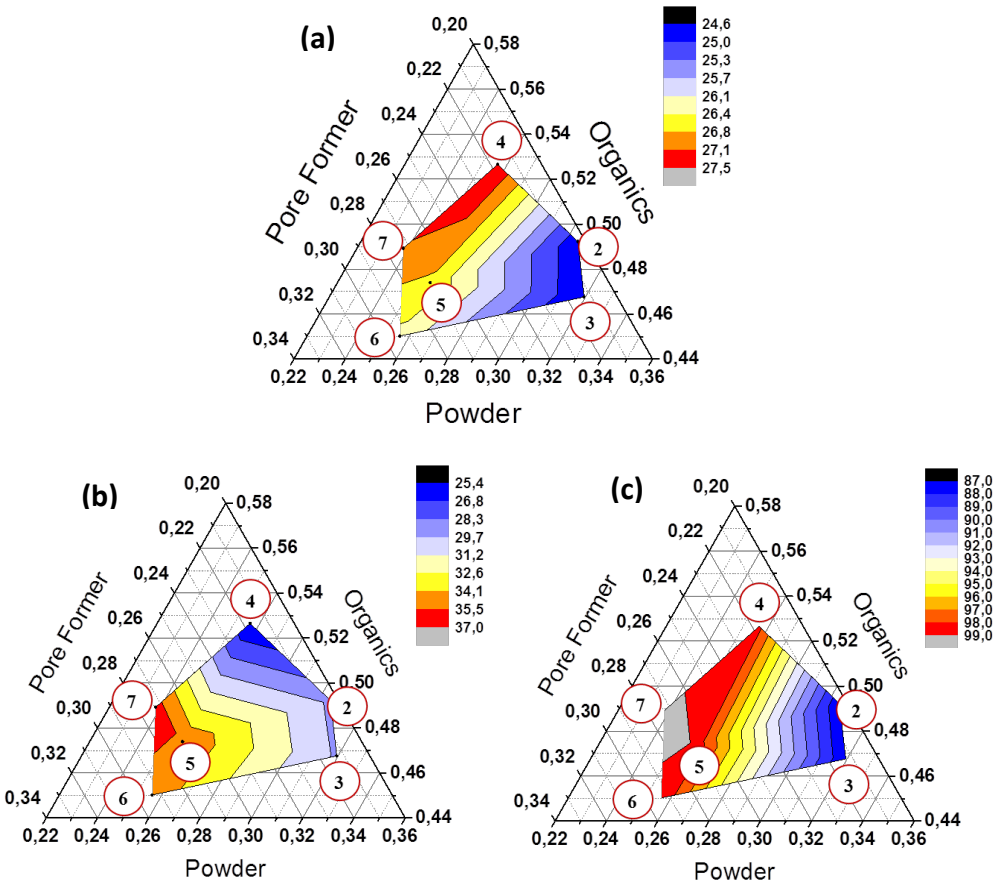

Figure 4 Ternary diagrams of the shrinkage (a), support porosity (b) and membrane density (c) of the sintered samples using different green support formulation. In the red circles are reported the number of the tape used as support.

2. *The amount of ZnO used as sintering aid in the membrane layer*

The role of the sintering aid was investigated to promote the membrane layer densification at lower sintering temperature, thus avoiding any BCZY-GDC interdiffusion issues that can take place via solid-state reaction at 1550 °C.

In this respect, three different amounts of ZnO were evaluated for the densification of the membrane layer, i.e. 0.7, 1 and 2 wt. % respect to the BCZY-GDC powders.

Figure 5 depicts the SEM micrographs of the polished cross-section of the membranes after sintering at 1550°C for four hours, with Tape 2, 4, and 7 as porous supports and with different ZnO content in the membrane layer.

Results showed that the 1 wt.% of ZnO enhanced the densification of the membrane layer. This effect was particularly appreciable for the Tape 2, which had the minor shrinkage percentage, indicating that the slight increase of the ZnO counterbalanced the limited shrinkage of the supporting layer. As the membrane shrinkage increased, the effect of the sintering aid content was less pronounced.

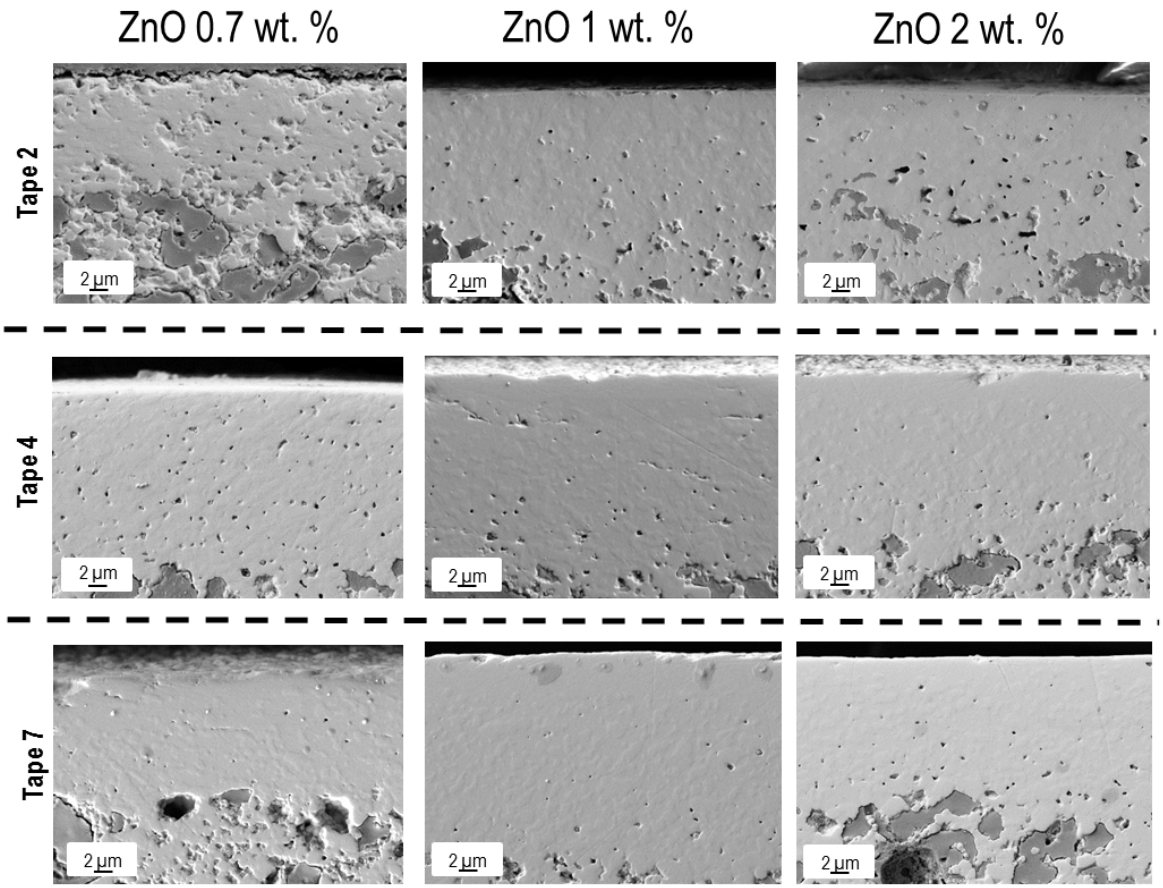

Figure 5 SEM micrographs of the polished cross-sections of the membranes sintered at 1550°C for four hours with different amount of sintering aid and using Tape 2, Tape 4 and Tape 7 as porous supports.

ZnO content higher than 1wt% did not significantly improve the densification of the membrane layer. Moreover, the use of 2 wt.% of ZnO, other than being useless, could be detrimental for the proton conductivity of the BCZY phase. In literature is reported [28-31] that the excess of Zn^{2+} in the perovskite lattice hinders the proton conductivity due to a proton-trapping effect. In fact, Zn^{2+} has the suitable radius ($r_{cationic}$ =0.74 Å) to replace the Zr^{4+} ($r_{cationic}$ = 0.72 Å) with a consequent formation of an effective -2 charge in the BO_6 octahedron which may be the responsible of the H^+ trapping:

$$ZnO \rightarrow Zn''_{Zr} + O_O + V''_{Ba} + 2\,V_{\ddot{O}} \qquad (1)$$

In conclusion, the asymmetric BCZY-GDC membrane formed by Tape 7 as support layer and the use of 1 wt.% of sintering aid in the active layer was found to represent the best combination for obtaining hydrogen separation membranes with suitable microstructure.

3. *Influence of the barium-source during sintering*

The nature of the sintering atmosphere plays a crucial role for the production of asymmetric BCZY-GDC membranes with the suitable microstructure, preserving, at the same time, the original perovskite-fluorite composite phase [22].

To avoid Ba loss from the membrane surface and preserve the BCZY perovskite structure, the use of a sacrificial Ba-source powder during the sintering treatment is mandatory.

Fig. 6 reports the SEM micrographs of the cross sections and the XRD spectrum collected on the top surface for the membrane sintered using BCZY as Ba source during the thermal treatments.

The use of BCZY as Ba source leads to a complete densification of the membrane but the formation of undesired single phase in the first 2-3 µm of the dense membrane. Fig. 6 (b) highlights the formation of a 2 ± 0.5 µm-thick BCZY layer (dark grey phase) on the top of the dense membrane,

while the two BCZY and GDC (light grey phase) distinct phases were still detected in the inner part of the membrane layer. This phenomenon is also confirmed by XRD analyses (Fig. 6 (c)) revealing that the dense surface is mainly composed by the perovskite BCZY phase, with a minor content (< 10%) of the fluorite GDC phase.

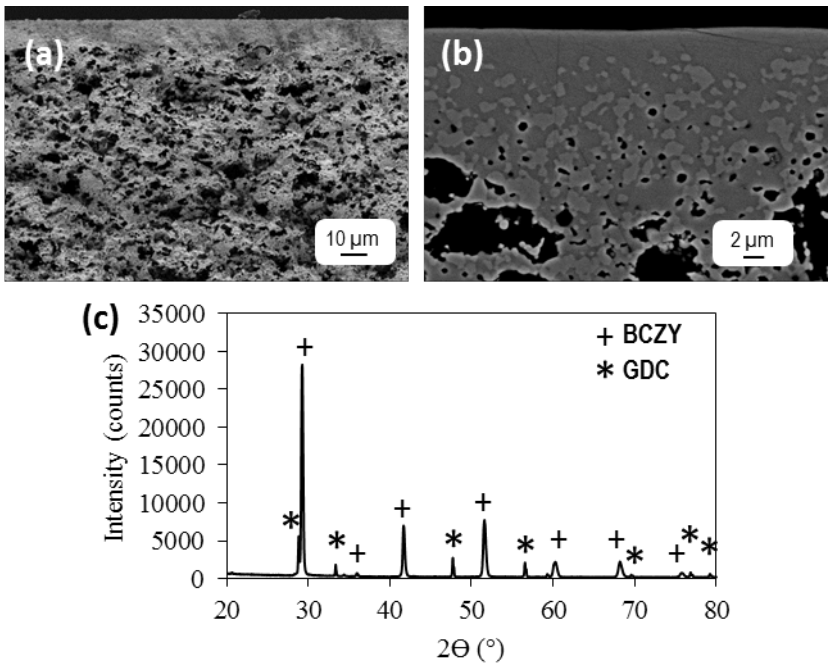

Figure 6 SEM micrographs of the fresh fracture (a) and of the polished cross section (b) of the BCZY-GDC membrane sintered at 1550°C for 4h using BCZY as Ba-source during the sintering process. XRD diffractogram performed onto the dense surface of the corresponding membrane (c).

Since the solid-state reaction takes place in the superficial portion of the membrane, a common strategy generally applied for bulk materials is the use of a polishing step to remove the undesired phase, obtaining a thinner membrane layer with the dual phase composition. The use of a mechanical abrasion was therefore evaluated checking the microstructure and composition of the membrane after different polishing steps with a SiC abrasive paper (Figure 7).

The as sintered membrane shows a layer of a 2.5 µm thick undesired single phase as confirmed by the correspondent XRD diffractogram. Only after the removal of 5 µm of materials, peaks ascribable to the fluorite GDC phase were detected. The most intense peak of the fluorite phase was

not detected, probably because covered by the BCZY most intense peak at 28.9°. After removal of 13 μm of material, the GDC peaks become more intense, and the most intense peak at 28.5° more evident. These data assessed a compositional gradient starting from the surface to the inner part of the dense membrane layer.

However, two drawbacks emerged following this procedure: i) the ratio (50:50) between the two phases of the cer-cer was not preserved as revealed by the XRD pattern obtained after the removal of 13 μm of material that shows that the fluorite phase content is lower than 25%; and ii) preliminary room-temperature He-leak tests showed that the polishing procedure is detrimental for the gas tightness of the membrane, making impractical the polishing process for the production of asymmetric membranes with the desired composition.

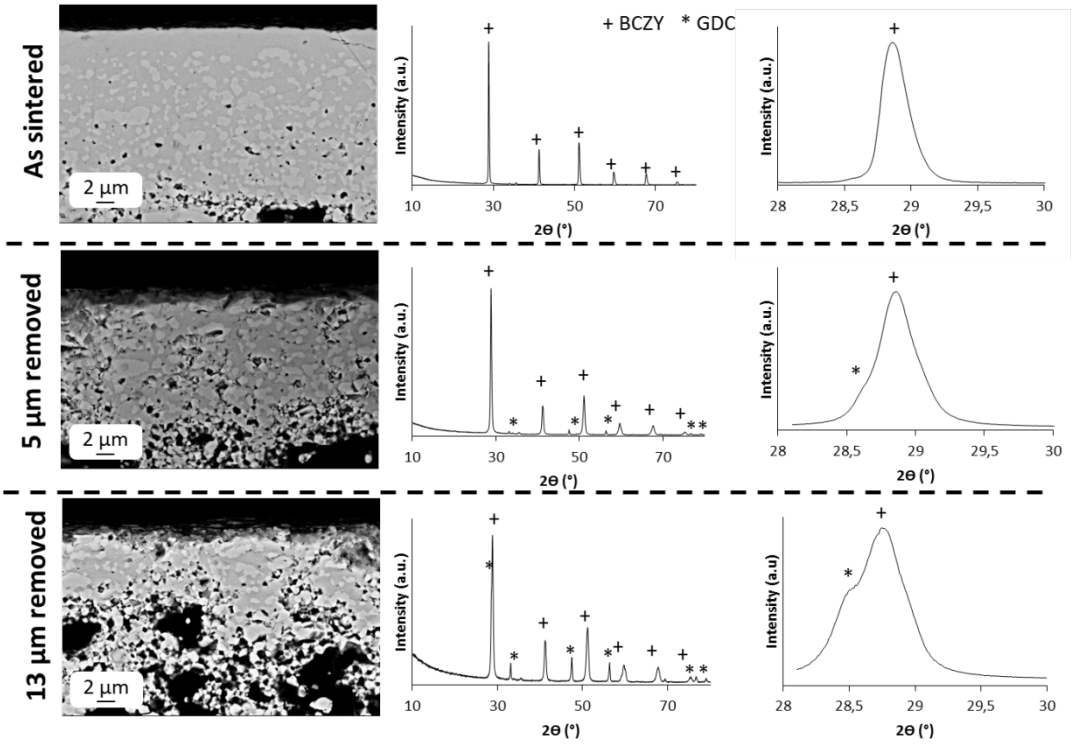

Figure 7 SEM micrographs of the polished fractures of the membranes as-sintered and after different steps of the abrasion process. XRD analyses performed on the dense surface after each polishing step are also reported on the side of the corresponding SEM micrograph.

The successful strategy to retain the fluorite-perovskite original composition was found to be the use of a less reactive powder (i.e. BCZY-GDC mixture) as Ba-source during the sintering step. Figure 8 reports the XRD spectrum of the membrane surface and SEM micrographs of the fresh fracture and polished cross section of the membrane sintered using the BCZY-GDC mixture as Ba-source during the sintering process. A gas tight, sufficiently dense 20 μm-thick cer-cer membrane layer supported by a porous (36 %) 750 μm-thick BCZY-GDC layer was obtained preserving the original dual-phase composition.

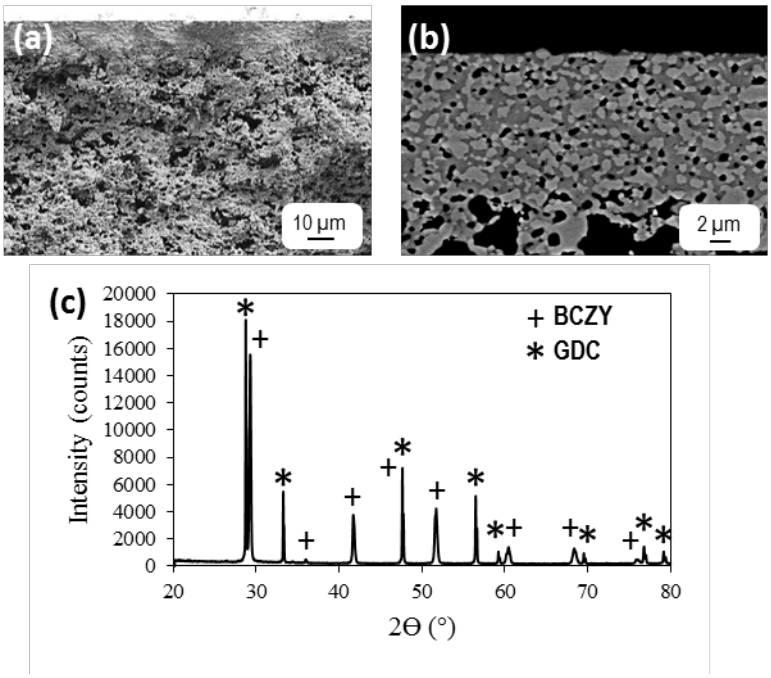

Figure 8 SEM micrographs of the fresh fracture (a) and of the polished cross section (b) of the BCZY-GDC membrane sintered at 1550°C for 4h using BCZY as Ba-source during the sintering process. XRD diffractogram performed onto the dense surface of the corresponding membrane (c).

Hydrogen permeations

Hydrogen permeation tests performed onto BCZY-GDC membranes supported on a porous substrate of the same composition and sintered with two different Ba-sources (i.e. BCZY or BCZY-GDC mixture) are reported in Figure 9. The H_2 flux (mL min^{-1} cm^{-2}) was recorded either as a function of the temperature and of the H_2 partial pressure in the feed side for both the membranes tested. Both streams, sweep and feed, were humidified (pH_2O=0.025 atm).

As expected, the H_2 flux increases with increasing temperature and H_2 partial pressure, as postulated by the Wagner equation, for both the membranes considered. The membrane sintered using BCZY as Ba-source and therefore constituted by an undesired 2-3 µm thick single phase on the top surface, shows at 750 °C H_2 fluxes of 0.045, 0.068 and 0.097 mL min^{-1} cm^{-2} feeding the 20, 50 and 80% of H_2 in He respectively. Even if the electrochemical characterization of the undesired layer was not possible, it can be assumed for it the same poor ambipolar conductivity of the doped barium cerate materials. In fact, the H_2 flux values of the membrane are close to those reported for asymmetric mixed proton electron conductor membranes (MPECs) [32-33], where the low electron conductivity limits the hydrogen permeation.

On the other hand the membrane sintered using BCZY-GDC mixture as Ba-source and therefore constituted by the perovskite-fluorite composite phase showed very promising H_2 permeability [34]. The H_2 fluxes registered at 750°C are 0.29, 0.47 and 0.58 mL min^{-1} cm^{-2} feeding the 20, 50 and 80% of H_2 in He respectively, roughly five times higher respect to the abovementioned ones.

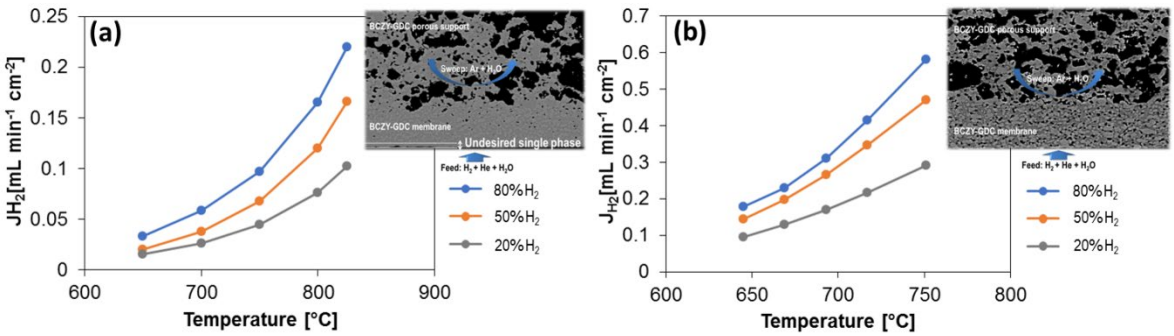

Figure 9 H_2 flux (mL min^{-1} cm^{-2}) as a function of temperature and H_2 partial pressure for membranes sintered at 1550 °C with BCZY (a) and BCZY-GDC (b) as barium source.

Conclusions

This work highlights for the first time the most critical issues related to the production of tape cast asymmetric BCZY-GDC membranes for hydrogen separation. It was demonstrated that a careful

balance of the pore former and organics amount in the green support layer formulation is of paramount importance to obtain a planar membrane constituted by a porous support and a thin active layer with the suitable microstructure. The composition of the green support layer in fact highly affects the sample shrinkage and, as a consequence, the densification of the membrane layer as well as the porosity of the substrate. The increase of the ZnO content from 0.7 wt % to 1 wt % enhanced the densification of the active layer while 2 wt. % of ZnO did not lead to any further improvement. A strict control of the sintering atmosphere is crucial in order to preserve the fluorite-perovskite composite phase within the whole membrane thickness. The ad-hoc production strategy reported in this work allowed to obtain planar and crack-free asymmetric membrane constituted by a sufficiently dense 20 μm-thick cer-cer layer supported by a porous (36 %) 750 μm-thick BCZY-GDC substrate. The asymmetric membranes here reported show H_2 fluxes among the highest obtained for an all-ceramic membrane, even higher than ceramic-Ni composites at similar conditions.

References

[1] Buonomenna MG, Bae J. Membrane processes and renewables energies. Renew. Sustainable Energy Rev. 2015; 43: 1343-1398.

[2] Noble RD, Stern SA. Membrane Separations Technology – Principles and Applications. Elsevier Science (1995) Amsterdam.

[3] X. Tan, X. Tan, N. Yang, B. Meng, K. Zhang, S. Liu, High performance BaCe0.8Y0.2O3-α (BCY) hollow fibre membranes for hydrogen permeation, Ceram. Int. 40 (2014) 3131–3138.

[4] J. Song, J. Kang, X. Tan, B. Meng, S. Liu, Proton conducting perovskite hollow fibre membranes with surface catalytic modification for enhanced hydrogen separation, J. Eur. Ceram. Soc. 36 (2016) 1669–1677.

[5] Z. Zhu, J. Hou, W. He, W. Liu, High-performance $Ba(Zr_{0.1}Ce_{0.7}Y_{0.2})O_{3-\delta}$ asymmetrical ceramic membrane with external short circuit for hydrogen separation, J. Alloy. Compd. 660 (2016) 231-234.

[6] S. Cheng, V.K. Gupta, J.Y.S. Lin, Synthesis and hydrogen permeation properties of asymmetric proton-conducting ceramic membranes, Solid State Ionics 176 (2005) 2653–2662.

[7] Montaleone D, Mercadelli E, Gondolini A, Pinasco P, Sanson A. On the compatibility of dual phase $BaCe_{0.65}Zr_{0.2}Y_{0.15}O_3$- based membrane for hydrogen separation application. Ceram. Intern. 2017; 43 (13): 10151–10157.

[8] H. Wang, X. Wang, B. Meng, X. Tan, K.S. Loh, J. Sunarso, S. Liu. Perovskite-based mixed protonic–electronic conducting membranes for hydrogen separation: Recent status and advances, J. Ind. Eng. Chem. 2018;60: 297-306.

[9] Adhikari S, Fernando S. Hydrogen membrane separation techniques. Ind. Eng. Chem. Res. 2006; 45: 875-881.

[10] Shang Y, Wei L, Meng X, Meng B, Yang N, Sunarso J, Liu S. CO_2-enhanced hydrogen permeability of dual-layered A-site deficient $Ba_{0.95}Ce_{0.85}Tb_{0.05}Zr_{0.1}O_{3-\delta}$-based hollow fiber membrane. J. Membr. Sci. 2018; 546: 82–89.

[11] Ivanova ME, Escolástico S, Balaguer M, Palisaitis J, Sohn YJ, Meulenberg WA, Guillon O, Mayer J, Serra JM. Hydrogen separation through tailored dual phase membranes with nominal composition $BaCe_{0.8}Eu_{0.2}O_{3-\delta}$:$Ce_{0.8}Y_{0.2}O_{2-\delta}$ at intermediate temperatures. Sci. Rep. 2016; 6: 34773.

[12] Rosensteel WA, Ricote S, Sullivan NP. Hydrogen permeation through dense $BaCe_{0.8}Y_{0.2}O_{3-\delta}$ – $Ce_{0.8}Y_{0.2}O_{2-\delta}$ composite-ceramic hydrogen separation membranes. Int. J. Hydrog. Energy. 2016; 41: 2598.

[13] Liu Y, Dai L, Zhang W, Zhou H, Li Y, Wang L. Preparation of dual-phase composite $BaCe_{0.8}Y_{0.2}O_3/Ce_{0.8}Y_{0.2}O_2$ and its application for hydrogen permeation. Ceram. Int. 2016; 42: 6391.

[14] Elangovan S, Nair BG, Small TA, Heck B. Ceramic mixed protonic/electronic conducting membranes for hydrogen separation. US Pat., US7258820 B2, 2007, Ceramatec inc. US.

[15] Rebollo E, Mortalò C, Escolastico S, Boldrini S, Barison S, Serra JM, Fabrizio M. Exceptional hydrogen permeation of all-ceramic composite robust membranes based on $BaCe_{0.65}Zr_{0.20}Y_{0.15}O_{3-\delta}$ and Y- or Gd-doped ceria, Energy Environ. Sci. 2015; 8: 3675-3686.

[16] Mortalò C, Rebollo E, Escolástico S, Deambrosis S, Haas-Santo K, Rancan M, Dittmeyer R, Armelao L, Fabrizio M. Enhanced sulfur tolerance of $BaCe_{0.65}Zr_{0.20}Y_{0.15}O_{3-\delta}$-$Ce_{0.85}Gd_{0.15}O_{2-\delta}$ composite for hydrogen separation membranes. J. Membrane Sci. 2018; 564: 123–132.

[17] Hamakawa S, Li L, Li A, Iglesia E. Synthesis and hydrogen permeation properties of membranes based on dense $SrCe_{0.95}Yb_{0.05}O_{3-\alpha}$ thin films. Solid State Ion. 2002; 148: 71–81.

[18] Gondolini A, Mercadelli E, Sangiorgi A, Sanson A. Integration of Ni-GDC layer on a NiCrAl metal foam for SOFC application. J. Eur. Ceram. Soc. 2017; 37 (3): 1023-1030.

[19] Viviani M, Canu G, Carpanese MP, Barbucci A, Sanson A, Mercadelli E, Nicolella C, Vladikova D, Stoynov Z, Chesnaud A, Thorel A, Ilhan Z, Ansar SA. Dual cells with mixed protonic-anionic conductivity for reversible SOFC/SOEC operation. Energy Procedia 2012; 28: 182-189.

[20] Mercadelli E, Gondolini A, Pinasco P, Sanson A. Stainless steel porous substrates produced by tape casting. Metals and Materials International 2017; 23 (1): 184-192.

[21] Mercadelli E, Sanson A, Pinasco P, Roncari E, Galassi C. Influence of carbon black on slurry compositions for tape cast porous piezoelectric ceramics. Ceram. Int. 2011; 37: 2143–2149.

[22] Montaleone D, Mercadelli E, Gondolini A, Ardit M, Pinasco P, Sanson A. Role of the sintering atmosphere in the densification and phase composition of asymmetric BCZY-GDC composite membrane. J. Eur. Ceram. Soc. 2019; 39: 21–29.

[23] Escolástico S, Solís C, Kjølseth C, Serra JM. Catalytic Layer Optimization for Hydrogen Permeation Membranes Based on $La_{5.5}WO_{11.25-\delta}/La_{0.87}Sr_{0.13}CrO_{3-\delta}$ Composites. ACS Applied Materials & Interfaces 2017; 9 (41): 35749-35756.

[24] Escolástico S, Somacescu S, Serra J.M. Tailoring mixed ionic–electronic conduction in H2 permeable membranes based on the system $Nd_{5.5}W_{1-x}Mo_xO_{11.25-\delta}$. J. Mater. Chem. A. 2015; 3(2): 719-731.

[25] Deibert W, Ivanova ME, Meulenberg WA, Vaßen R, Guillon O. Preparation and sintering behavior of $La_{5.4}WO_{12-\delta}$ asymmetric membranes with optimized microstructure for hydrogen separation. J. Membr. Sci. 2015; 492: 439-451.

[26] Zhan S, Zhu X, Ji B, Wang W, Zhang X, Wang J, Yang W, Lin L. Preparation and hydrogen permeation of $SrCe_{0.95}Y_{0.05}O_{3-\delta}$ asymmetrical membranes. J. Membr. Sci. 2009; 340: 241–248.

[27] Mercadelli E, Montaleone D, Gondolini A, Pinasco P, Sanson A. Tape-cast asymmetric membranes for hydrogen separation. Ceram. Int. 2017; 43: 8010-8017.

[28] Babilo P, Haile SM. Enhanced sintering of yttrium-doped barium zirconate by addition of ZnO. J. Am. Ceram. Soc. 2005; 88: 2362-2368.

[29] Zhang C, Zhao H, Xu N, Li X, Chen N. Influence of ZnO addition on the properties of high temperature proton conductor $Ba_{1.03}Ce_{0.5}Zr_{0.4}Y_{0.1}O_{3-d}$ synthesized via citrate-nitrate method. Int. J. Hydrogen Energy 2009; 36: 2739-2746.

[30] Peng C, Melnik J, Luo J, Sanger AR, Chuang KT. $BaZr_{0.8}Y_{0.2}O_{3-\delta}$ electrolyte with and without ZnO sintering aid: preparation and characterization. Solid State Ionics 2010; 181: 1372-1377.

[31] Ricote S, Bonanos N, Manerbino A, Coors WG. Conductivity study of dense $BaCe_xZr_{(0.9-x)}Y_{0.1}O_{(3-d)}$ prepared by solid state reactive sintering at 1500°C. Int. J. Hydrogen Energy 2012; 37: 7954-7961.

[32] Wei Y, Xue J, Wang H, Caro J. Hydrogen permeability and stability of $BaCe_{0.85}Tb_{0.05}Zr_{0.1}O_{3-\delta}$ asymmetric membranes. J. Membr. Sci. 2015; 488: 173-181.

[33] Sun W, Shi Z, Liu W. Considerable Hydrogen Permeation Behavior through a Dense $Ce_{0.8}Sm_{0.2}O_{2-\delta}$ (SDC) Asymmetric Thick Film. J. Electrochemical Soc. 2013; 160: F585-F590.

[34] Montaleone D, Mercadelli E, Escolàstico S, Gondolini A, Serra JM, Sanson A. All-ceramic asymmetric membranes with superior hydrogen permeation. J. Mater. Chem. A. 2018; 6: 15718.